Available online at www.sciencedirect.com
ScienceDirect
Trans. Nonferrous Met. Soc. China 32(2022) 2709−2718
Transactions of Nonferrous Metals Society of China
www.tnmsc.cn

Synthesis of novel thionocarbamate for copper−sulfur flotation separation and its adsorption mechanism

Fei CAO[1,2], De-si SUN[1], Xian-hui QIU[3,4], De-zhi ZHOU[1], Xing-rong ZHANG[2], Chuan-yao SUN[2]

1. School of Chemistry and Chemical Engineering, Jiujiang University, Jiujiang 332005, China;
2. State Key Laboratory of Mineral Processing, BGRIMM Technology Group, Beijing 102600, China;
3. School of Resource and Environment Engineering,
Jiangxi University of Science and Technology, Ganzhou 341000, China;
4. State Key Laboratory of Comprehensive Utilization of Low-Grade Refractory Gold Ores
(Zijin Mining Group Co., Ltd.), Shanghang 364200, China

Received 29 July 2021; accepted 18 January 2022

Abstract: As a novel collector, O-isopropyl-N,N-diethyl thionocarbamate (IPDTC) was designed and synthesized for copper−sulfur flotation separation. Density functional theory calculations were performed to investigate the electronic structures of IPDTC. The results showed that IPDTC had higher energy of the highest occupied molecular orbital but lower electronegativity than O-isopropyl-N-ethyl thionocarbamate (Z−200). It was predicted that IPDTC had strong collection ability according to the reaction energy criteria. Flotation results demonstrated that the collecting ability of IPDTC to chalcopyrite and pyrite was stronger than that of Z−200. Then, the flotation mechanism was analyzed by measurements of surface tension, adsorption capacity, XPS, FTIR and zeta potential. These results indicated that IPDTC could reduce the solution surface tension. The adsorption capacity of IPDTC on chalcopyrite was higher than that on pyrite, consistent with the results of the flotation tests. FTIR, zeta potential and XPS results also demonstrated that IPDTC was strongly absorbed on the chalcopyrite surface by formation of Cu—S—C bonds, but showed a weak affinity on the pyrite surface.

Key words: O-isopropyl-N,N-diethyl thionocarbamate; adsorption mechanism; chalcopyrite; pyrite; density functional theory

1 Introduction

Copper−sulfur flotation separation is one of the difficulties in sulfide ore flotation. Therefore, the design of suitable flotation collectors is an important direction to resolve the problem of flotation separation [1−3]. As is known, xanthate is commonly used as a collector in the industry. However, under the condition of high alkalinity with a large amount of lime, there are some disadvantages, such as blocked equipment pipes and inhibited pyrite activation difficulty. With increasing refractory copper sulfide ores, thionocarbamate collectors are generally used as an alternative to xanthate [4,5], because thionocarbamate collectors show better selectivity than xanthate. However, their collecting ability is not as good as that of xanthate [6,7]. To enhance the efficiency of copper−sulfur separation, it is very important to develop collectors with both collecting ability and selectivity for chalcopyrite under low alkali conditions [8,9]. Therefore, the relation between flotation performance and the molecular structure of the collector must be uncovered [10−15]. For example, if the electron donor group is introduced

Corresponding author: Fei CAO, Tel: +86-15107929378, E-mail: jjyz2001@163.com
DOI: 10.1016/S1003-6326(22)65977-6

into collectors, how would the flotation performance of Z−200 change? Will the adsorption capacity of the collectors on chalcopyrite surfaces be enhanced? The traditional treatment method is to carry out a flotation test to explore new collectors and then use quantum chemistry, Fourier transform infrared (FTIR), adsorption capacity measurement, zeta potential, and X-ray photoelectron spectroscopy (XPS) to investigate interaction mechanisms between the collector and minerals [16−23]. However, this method is time-consuming and costly. Instead, by adopting theoretical methods (such as the interaction energy criterion and frontier orbital theory) to design novel collectors, flotation verification tests and flotation mechanism research can be executed [24−26]. As a result, this way not only screens out some collectors with good flotation performance in advance, lessens the number of flotation tests and enhances targeting, but also shortens the research period and costs.

In this work, the structure of Z–200 was modified via replacing the hydrogen atom connected to the N atom in Z–200 by an ethyl group to construct a new type structure as O-isopropyl-N,N-diethyl thionocarbamate (IPDTC). First, density functional theory (DFT) was employed to calculate the quantum chemistry of IPDTC and Z–200 [27]. By analyzing the frontier orbital properties such as the highest occupied molecular orbital (HOMO), and using the interaction energy criterion, flotation performance of IPDTC molecules was predicted. The target molecules as collectors were then synthesized and tested for flotation. The adsorption capacity, FTIR, surface tension, zeta potential and XPS were measured to reveal the flotation mechanism of the collector.

2 Experimental

2.1 Materials

Single minerals of chalcopyrite and pyrite were obtained from Hubei Province, China. The minerals were crushed, handpicked, ground and sieved. The fraction with sizes of 0.038−0.074 mm was used for pure mineral flotation tests.

The IPDTC synthesis was executed in two steps. First, sodium chloroacetate and sodium isopropyl xanthate were adopted as raw materials to produce the intermediate isopropyl xanthate sodium acetate at 35 °C and pH 8 for 2 h. The product of O-isopropyl-N,N-diethyl thionocarbamate was obtained via the aminolysis reaction of the intermediate with diethyl amine at 40 °C for 4 h. The yield of IPDTC was 78.6%, the purity of IPDTC was 99.2% by GC analysis, and the structure of IPDTC was characterized by NMR (^{1}H NMR (400 MHz, MeOD) δ: 1.15 (t, 3H, CH_2CH_3), 1.20 (t, 3H, CH_2CH_3), 1.30 (d, 6H, $CHCH_3$), 3.48 (q, 2H, NCH_2CH_3), 3.81 (q, 2H, NCH_2CH_3), 5.56 (m, 1H, $OCH(CH_3)_2$) 10^{-6}; ^{13}C NMR (100 MHz, MeOD) δ: 12.2 (s, 1C, CH_3), 13.5 (s, 1C, CH_3), 22.1 (s, 2C, CH_3), 44.2 (s, 1C, CH_2), 48.4 (s, 1C, CH_2), 75.3 (s, 1C, CH), 187.8 (s, 1C, C═S) 10^{-6}).

2.2 Computational methods

The molecular structures of IPDTC and Z−200 were optimized by applying Gaussian 09 software at the B3LYP level, 6-31G(d) basis set [28]. The solvation effect of water was examined by using integral equation formalism for the polarizable continuum (IEF-PCM) model. According to Koopmans' approximation, electronegativity (χ) could be calculated on the basis of the following formula [29]:

$$\chi=-(E_{HOMO}+E_{LUMO})/2 \quad (1)$$

where E_{HOMO} and E_{LUMO} are the highest and the lowest unoccupied molecular orbital energies, respectively.

2.3 Flotation experiments

The pure mineral flotation experiments were conducted in an XFG II5 flotation apparatus. The mineral with a total of 2.00 g (0.038−0.074 mm) was cleaned ultrasonically for 3 min. As-cleaned samples were poured into a 50 mL flotation cell and stirred for 2 min. After adjusting the pulp pH, flotation was operated for 5 min. Then, the dried concentrates and tailings were weighed separately, and the concentrate recovery was calculated. To minimize the experimental error, three parallel experiments were completed to obtain an average value. The standard deviation of parallel experiments is expressed in the form of error bars.

2.4 Surface tension experiments

Surface tension was measured by using a JYW−200B meter (Hebei Jinhe, China). The collector solutions were prepared using triple distilled water. Pure minerals (1.00 g) with particle

size of 0.038−0.074 mm were put into a small beaker and ultrasonically cleaned for 3 min, and later, the upper water was poured out. Then, 50 mL of collector solution was added, stirred for 30 min, and finally filtered. The surface tension of the filtrate was measured three times for average statistics.

2.5 Adsorption capacity experiments

In this test, the absorbance of collector solutions was measured using ultraviolet and visible spectrophotometers, and a standard curve of concentration and absorbance was made for the collector. All data were measured three times to obtain an average value. Pure mineral of 1.00 g was cleaned with ultrasonication for 3 min, followed by placing into flotation cell of 50 mL and stirring for 30 min. The upper supernatant was removed after centrifugation, and the absorbance of the supernatant was measured. Finally, the residual concentration of the collector was calculated utilizing the standard curve. The equilibrium adsorption capacity, Q_e (mol/m^2), of the collector with minerals was calculated by the following formula:

$$Q_e = \frac{(c_0 - c_e)V}{mS} \tag{2}$$

where c_0 and c_e represent the initial and equilibrium concentrations (mol/L) of the collector before and after adsorption, respectively. V, m and S represent the volume (L) of the solution, the mass (g) of the mineral and the surface area (m²/g) of the mineral, respectively. The BET surface area of pyrite (2.31 m²/g) is larger than that of chalcopyrite (1.53 m²/g).

2.6 FTIR measurements

During the experiment, single mineral samples were ground to <5 μm with agate grinders. At the beginning, the samples were ultrasonically cleaned for 3 min and poured into the flotation cell. Thereafter, the collector and pH modifying agent (pH=9.0) were added. The flotation pulp was stirred for 10 min, filtered, washed 3 times, and dried in vacuum. Finally, as-prepared samples were used to conduct FTIR measurements.

2.7 Zeta potential measurement

The zeta potentials of mineral samples before and after IPDTC treatment were determined by a ZetaPlus zeta potential analyzer (Brookhaven Instruments, USA). In each test, samples of 40 mg (<5 μm) were added to KCl aqueous solution (50 mL, 1×10^{-3} mol/L). Concentration of IPDTC was 20 mg/L. The pH of the suspension was adjusted with NaOH or HCl solution. After stirring the suspension for 15 min, the zeta potential was measured. The average value of five parallel measurements was taken as the zeta potential.

2.8 XPS analysis

A Thermo Fisher Escalab 250Xi spectrometer (Thermo Fisher, USA) was used to measure the XPS spectra of chalcopyrite before and after interaction with IPDTC. A total of 1.00 g of <0.038 mm chalcopyrite samples was added to IPDTC aqueous solution. The suspension was stirred for 15 min at pH 9.0. The measurement was conducted at 150 W with pass energy of 20 eV and monochromatic Al K_α X-ray source. The binding energies were calibrated by using C 1s (284.8 eV).

3 Results

3.1 DFT calculations

To predict the flotation performance of IPDTC, the electronic structures of IPDTC and Z−200 were calculated by DFT. The calculated frontier molecular orbital energy (E_{HOMO} and E_{LUMO}), electronegativity (χ) and atomic NPA charge of the collectors are listed in Table 1. Frontier molecular orbital shapes of the collectors are shown in Fig. 1. The HOMOs of IPDTC and Z–200 molecules are mainly composed of π bonds of C═S double bonds, while the LUMOs consist of π* anti-bond orbitals of C═S. Therefore, it is inferred that the double bond S atom is the bonding atom of thionocarbamate. The HOMO shapes of IPDTC and Z−200 molecules match the d-orbital symmetry of metal ions, indicating that they have the conditions to form covalent bonds.

3.2 Prediction of flotation performance

The frontier orbital theory can explain the strength of the chemical bond between thionocarbamate and sulfide ore. On the premise of symmetry matching, according to Klopman's generalized perturbation theory, the expression of ΔE is shown as follows [30−32]:

Table 1 Properties of IPDTC and Z–200

Species	NPA atomic charge		E_{HOMO}/eV	E_{LUMO}/eV	ΔE_{H-L}/eV	Electronegativity/eV
	S	N				
IPDTC	−0.373	−0.468	−6.168	−0.533	5.635	3.350
Z−200	−0.378	−0.630	−6.336	−0.599	5.738	3.466

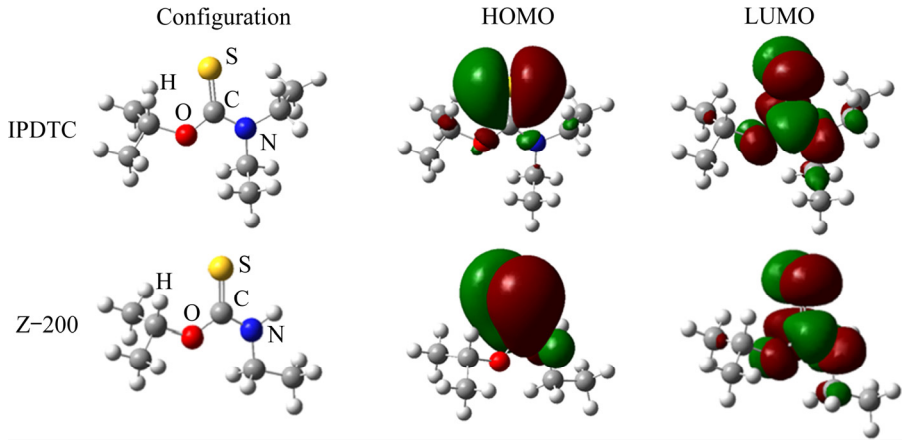

Fig. 1 Frontier orbital shapes of IPDTC and Z−200

$$\Delta E = -q_r q_s \frac{\Gamma}{\varepsilon} + \Delta_{solv} + \sum_{\substack{m \\ occ}} \sum_{\substack{n \\ unocc}} \left[\frac{2(c_r^m)^2 (c_s^m)^2 \beta^2}{E_m^* - E_n^*} \right] + \sum_{\substack{m \\ occ}} \sum_{\substack{n \\ unocc}} \left[\frac{2(c_r^m)^2 (c_s^m)^2 \beta^2}{E_n^* - E_m^*} \right] \quad (3)$$

where q_r and q_s represent total initial charges; Γ represents coulomb repulsion term; ε represents local dielectric constant of solvent; Δ_{solv} represents desolvation energy; c_r^m and c_s^n represent electron densities of the frontier orbital; β represents extent of bonding in transition state; "occ" represents occupied orbitals; "unocc" represents unoccupied orbitals; $(E_m^* - E_n^*)$ and $(E_n^* - E_m^*)$ represent the energy difference of frontier orbitals between collector and mineral [30,31]. The first item of ΔE indicates electrostatic action, the third item indicates that HOMO electrons of the collector are transferred to the LUMO of the mineral surface to form a normal covalent bond, and the fourth term indicates that the HOMO electrons of the mineral surface are transferred to the collector LUMO to form a feedback π bond. When $(E_m^* - E_n^*)$ is small, the value of the third term in ΔE is large, and the electron transfer between collector and mineral is important.

The NPA charge (q_r and q_s) of bonding atoms S reflects the electrostatic interaction between collectors and minerals. The HOMO energy (E_{HOMO}) of collectors determines the strength of the covalent bond between the collector and mineral (electrons transferred from collector to mineral). E_{HOMO}, natural population analysis (NPA) charge, and electronegativity (χ) of collectors are applied to predicting their flotation properties.

The smaller the NPA charge of the bonding atom in the collector molecule is, the stronger the electrostatic interplay between sulfide minerals and the collector is, suggesting that the collector shows strong collecting ability. The order of the NPA charge of the bonding atoms (S) of IPDTC and Z−200 follows Z−200 (−0.378) < IPDTC (−0.373), although the difference is small. It is inferred that the collecting ability of Z−200 is slightly higher than that of IPDTC.

As shown in Fig. 2, the larger the E_{HOMO} of the collector is, the closer it is to the E_{LUMO} of the mineral, as well as the stronger the covalent bond between the mineral and collector is, which indicates that the collector shows strong collecting

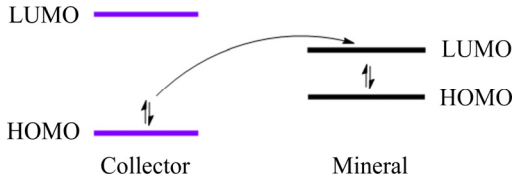

Fig. 2 Electron transfer diagram of interaction between collector and mineral

capacity for the mineral. In this work, the strength of covalent bonds of different collectors with the same mineral was studied, while the E_{LUMO} of the mineral remained unchanged. Therefore, the collecting ability can be inferred from the E_{HOMO} of collectors. The order of their E_{HOMO} is IPDTC (−6.168 eV) > Z−200 (−6.336 eV), indicating that the order of the collecting ability for chalcopyrite and pyrite is IPDTC > Z−200.

If the electronegativity (χ) of the collector molecule is smaller, the force between the collector and mineral is stronger, leading to strong collecting ability. Table 1 shows that the order of electronegativity of collectors is IPDTC (3.350 eV) < Z−200 (3.466 eV), suggesting that the order of the collecting capacity for chalcopyrite and pyrite is IPDTC > Z−200.

3.3 Flotation test results

Figure 3 shows that the flotation recoveries of chalcopyrite and pyrite were affected by the dosages of IPDTC and Z−200 at natural pH 5.6. The recovery of flotation chalcopyrite with IPDTC was 93.27%−98.46%, which was higher than that in the presence of Z−200 (82.53%−93.50%). The recovery of pyrite increased from 71.71% to 87.47% when IPDTC was used, which was also higher than that with Z−200 as the collector increased from 63.06% to 80.33%. The flotation result demonstrated that the collecting capacity of IPDTC for chalcopyrite and pyrite was stronger than that of Z−200, consistent with our previous predictions. The recovery of chalcopyrite or pyrite increased with increasing collector dosage, as shown in Fig. 3.

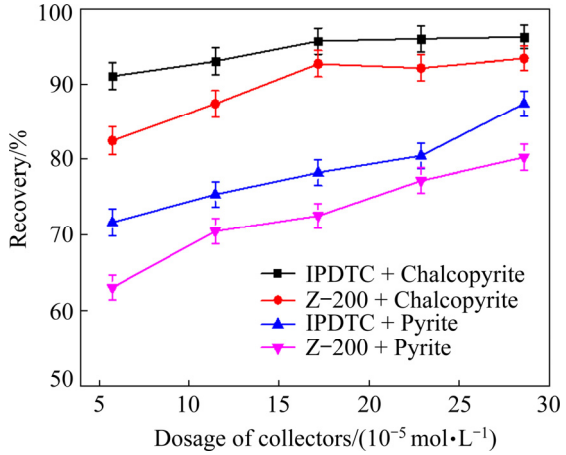

Fig. 3 Effect of collector dosage on flotation test results of IPDTC and Z−200 (pH=5.6)

When collector dosage was 5.71×10^{-5} mol/L, the influence of pH on the recovery of minerals is shown in Fig. 4. As the pulp pH increased, the collectors had strong collecting capacity for chalcopyrite, and the recovery of IPDTC (above 94.27%) was higher than that of Z−200 (86.553%−80.38%). This indicates that pH (6−11) had slight impact on the flotation recovery of chalcopyrite. However, the recovery of pyrite descended rapidly with increasing pH and descended slightly when the pH reached 9.0. This demonstrated that IPDTC had strong collecting ability and good selectivity under low-alkali conditions; therefore, it could be utilized as a novel high-efficiency collector.

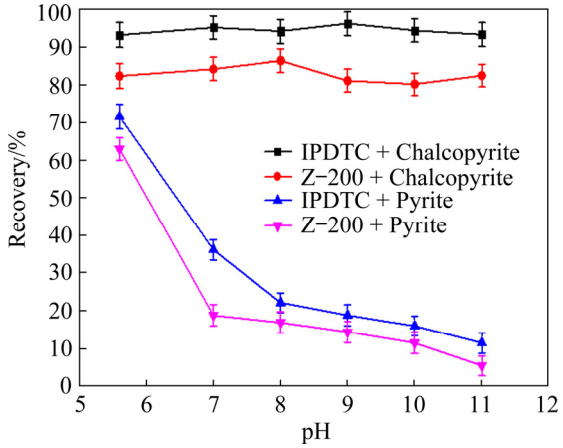

Fig. 4 Effect of pH on flotation test results of IPDTC and Z−200 (collector dosage of 5.71×10^{-5} mol/L)

3.4 Flotation mechanisms

3.4.1 Results of surface tension

The surface tension of triple distilled water was 72.74 mN/m at 20 °C. IPDTC could decrease the surface tension of water. The surface tension of the IPDTC liquor gradually decreased from 70.65 to 57.98 mN/m when the IPDTC concentration increased from 1.14×10^{-5} to 22.86×10^{-5} mol/L, as shown in Fig. 5(a). IPDTC reduced the surface tension of water more than Z−200. It did not decrease when the concentration increased to 17.14×10^{-5} mol/L. The surface tension of IPDTC solution (5.71×10^{-5} mol/L) was measured before and after the interaction with chalcopyrite. As shown in Fig. 5(b), the change in the surface tension of the IPDTC liquor increased from 62.14 to 64.86 mN/m. The increase in the surface tension after adsorption means that the remaining collector content in the solution was smaller, and some of

them were adsorbed on chalcopyrite. However, there was little change in the surface tension of the IPDTC solution before and after the interaction with pyrite. The results indicated that IPDTC could be adsorbed strongly on chalcopyrite.

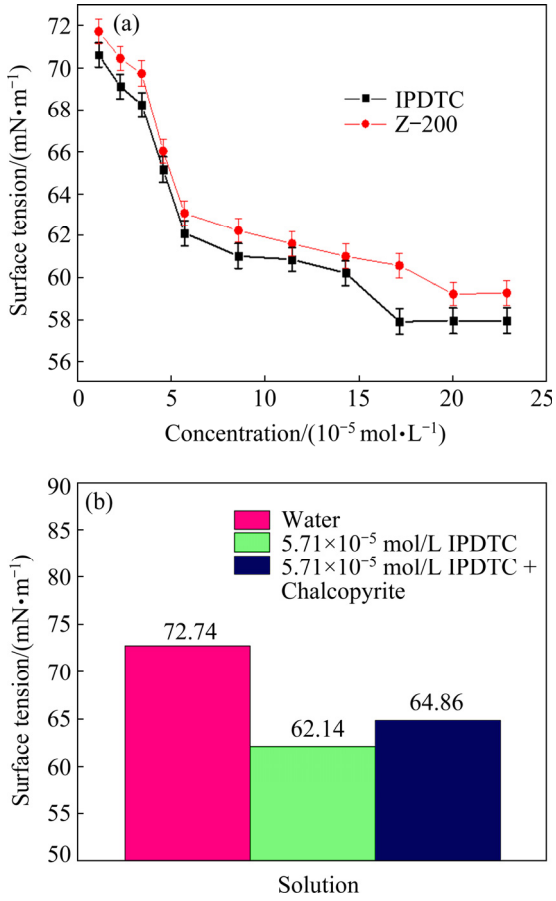

Fig. 5 Surface tension of IPDTC (a) and after interaction with chalcopyrite (b)

3.4.2 Adsorption capacity

According to the flotation tests of single minerals, IPDTC shows better selectivity at pulp pH 9.0. Therefore, we measured the adsorption of IPDTC with chalcopyrite and pyrite at pH 9.0 and calculated the adsorption amount (Q_e) according to the concentration change in IPDTC before and after adsorption, as shown in Fig. 6. As the IPDTC concentration increased, the adsorption capacity of IPDTC on chalcopyrite increased from 0.04×10^{-6} to 0.58×10^{-6} mol/m^2. However, the adsorption capacity of IPDTC on pyrite was small ($(0.005-0.054)\times10^{-6}$ mol/m^2), and the adsorption capacity slightly changed with increasing IPDTC concentration. The change in adsorption capacity was insignificant when the concentration increased to 11.42×10^{-5} mol/L. Under pH 9.0, IPDTC showed good selectivity, in agreement with the surface tension tests and pure mineral flotation tests.

As shown in Fig. 6, when the concentration of IPDTC was 11.42×10^{-5} mol/L, the adsorption ability of IPDTC for chalcopyrite was stronger than that for pyrite. This concentration was chosen to measure the adsorption capacity of IPDTC on chalcopyrite or pyrite at different pulp pH values (see Fig. 7). As the pH increased, the adsorption capacity of IPDTC to chalcopyrite slightly changed (from 0.52×10^{-6} to 0.50×10^{-6} mol/m^2), and the adsorption capacity of IPDTC to pyrite gradually declined. Thus, IPDTC could separate chalcopyrite and pyrite under low-alkali conditions.

3.4.3 FTIR results

Figures 8 and 9 show the FTIR spectra of chalcopyrite and pyrite before and after IPDTC treatment, respectively. As shown in Fig. 8, the FTIR spectrum of IPDTC after interacting with chalcopyrite was similar to that of IPDTC and showed obvious changes compared with the

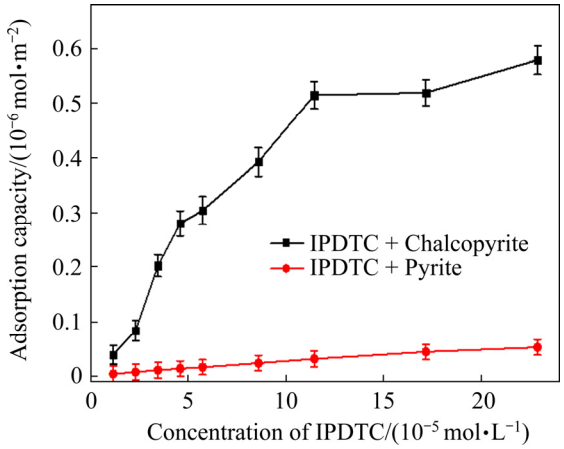

Fig. 6 Relationship between concentration of IPDTC and adsorption amount of pure minerals

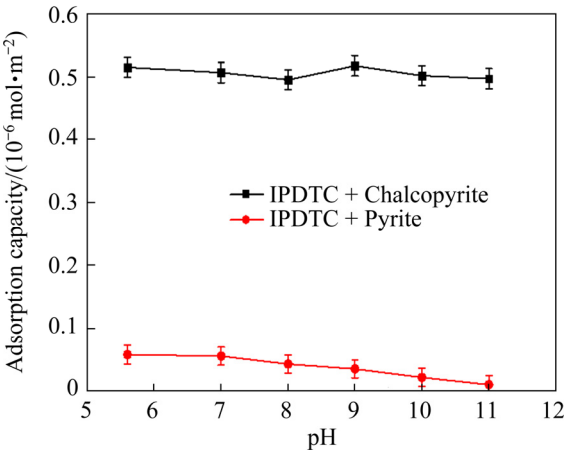

Fig. 7 Effect of pH on adsorption of IPDTC for mineral

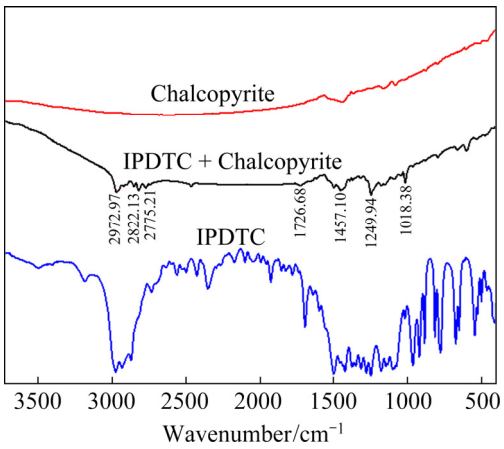

Fig. 8 FTIR spectra of chalcopyrite before and after IPDTC treatment (pH=9)

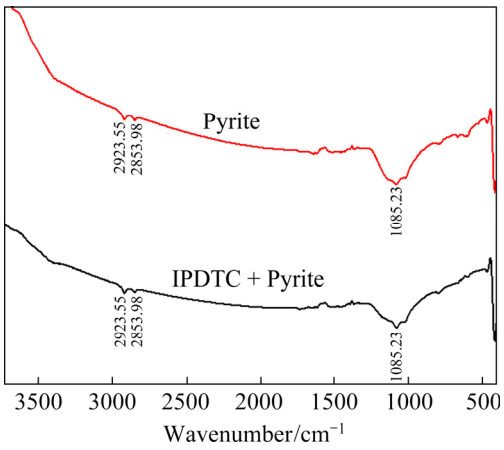

Fig. 9 FTIR spectra of pyrite before and after IPDTC treatment (pH=9)

spectrum of chalcopyrite before flotation. After the interaction of chalcopyrite and IPDTC, there were —CH_3 and —CH_2 stretching vibration absorption peaks at 2972.97, 2822.13 and 2775.21 cm^{-1}, C═S absorption peaks at 1726.68 cm^{-1}, C — O — C absorption peaks at 1249.94 cm^{-1}, C—N absorption peaks at 1018.38 cm^{-1}, and C—H bending vibration absorption peaks at 1457.10 cm^{-1}, demonstrating that IPDTC showed stronger adsorption on the chalcopyrite surface. However, the FTIR spectra of pyrite and IPDTC in Fig. 9 are changed insignificantly. It was inferred that IPDTC showed stronger interaction on the chalcopyrite surface at pH 9 but had no obvious adsorption on the pyrite surface, in agreement with our previous test results.

3.4.4 Zeta potential

When the mineral surface adsorbs collector, charge properties will change significantly [33,34]. Zeta potential can indicate the charge changes of mineral surfaces. Figure 10(a) shows that, after the interaction of chalcopyrite with IPDTC, the isoelectric point (IEP) of the chalcopyrite surface decreased from 4.64 to 4.07 mV. Under pH 2.0−12.0, the zeta potential of the chalcopyrite surface lessened significantly after IPDTC treatment, indicating that IPDTC had strong adsorption on the chalcopyrite surface. For pyrite, when interacting with IPDTC, the zeta potential was basically unchanged (see Fig. 10(b)), indicating that IPDTC adsorption on the pyrite surface was very weak. This also confirms our previous experimental results that IPDTC has strong collecting ability for chalcopyrite and weak ability for pyrite.

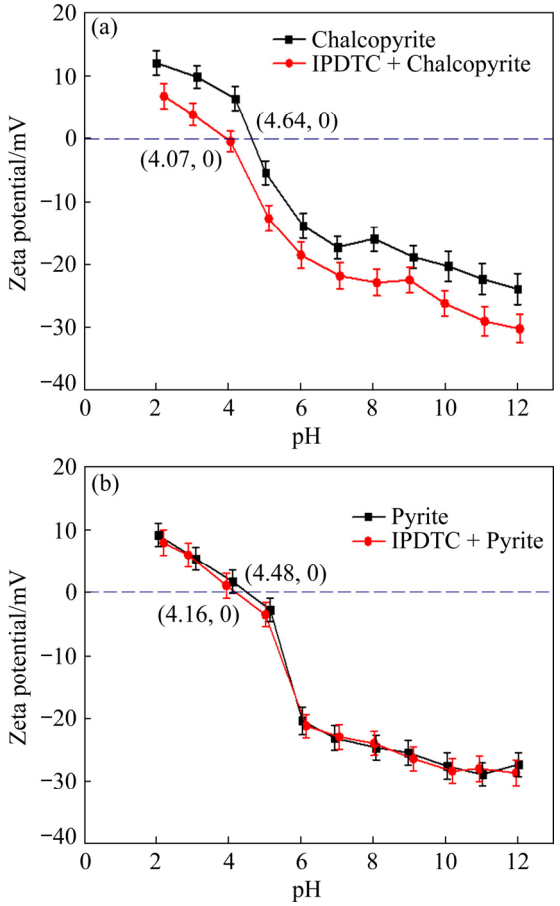

Fig. 10 Zeta potentials of chalcopyrite (a) and pyrite (b) before and after interaction with IPDTC

3.4.5 XPS results

The XPS spectra of chalcopyrite in the absence and presence of IPDTC are displayed in Fig. 11. The Cu 2p peaks at 932.28 and 931.88 eV of untreated chalcopyrite with IPDTC belong to $CuFeS_2$ and CuS, respectively [33]. After IPDTC treatment, the binding energies of these two Cu 2p peaks increased to 932.43 and 932.20 eV. The

increase in binding energy indicated that the electronic density of copper ions on the chalcopyrite surface decreased, which might be due to the electron transfer of copper ions to the bonding atoms in the IPDTC molecule.

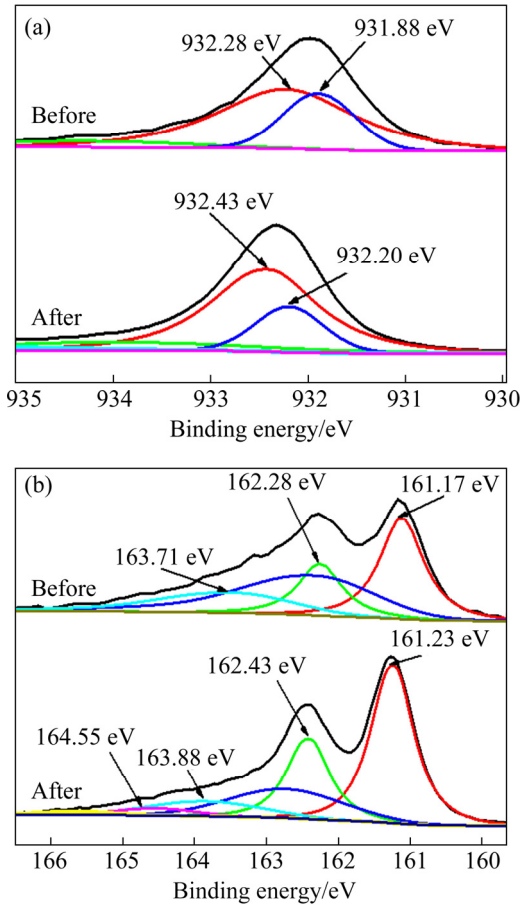

Fig. 11 Cu 2p (a) and S 2p (b) XPS spectra of chalcopyrite before and after IPDTC treatment

The S 2p spectrum of chalcopyrite before interaction at 161.17, 162.28 and 163.71 eV had three characteristic peaks. After treatment with IPDTC, the binding energy increased slightly to 161.23, 162.43 and 163.88 eV. Moreover, a new S 2p peak appeared at 164.55 eV after interaction of the chalcopyrite with IPDTC. The peak might be assigned to the Cu—S—C bond that was formed by Cu on the chalcopyrite surface with S atoms in the IPDTC molecule [7]. It was reasonable to infer that chemisorption occurred between chalcopyrite and IPDTC.

4 Conclusions

(1) An electron donor group (ethyl) was introduced into the Z−200 molecule, and two ethyl groups were connected to the N atom in IPDTC. Based on DFT calculations, it was predicted that the electron donor ability was enhanced, the E_{HOMO} value was larger than that of Z−200, the electronegativity was smaller than that of Z−200, and the collecting ability would be stronger.

(2) The flotation experiments demonstrated that IPDTC had strong collecting ability, confirming our theoretical prediction. Under low-alkali conditions, IPDTC had strong collecting ability for chalcopyrite but weak collecting ability for pyrite. The surface tension test supported this result as well.

(3) The adsorption capacity results further showed that as the concentration of collector increased, the adsorption capacity of IPDTC on chalcopyrite increased, while that on the pyrite surface was insignificantly changed. Moreover, pH did not affect the adsorption capacity of IPDTC on the chalcopyrite surface but had obvious negative effect on the pyrite surface.

(4) FTIR, XPS and zeta potential analyses also indicated that IPDTC might have strong chemical adsorption on the chalcopyrite surface but showed no adsorption on the pyrite surface. This further confirmed that the prediction of IPDTC flotation performance was accurate.

Acknowledgments

The authors are grateful for the financial supports from the Open Foundation of State Key Laboratory of Mineral Processing, China (Nos. BGRIMM-KJSKL-2019-06, BGRIMM-KJSKL-2022-13); the Open Fund of State Key Laboratory of Comprehensive Utilization of Low-Grade, China (No. ZJKY2017(B)KFJJ003).

References

[1] DOUGLAS W F, PRADIP. A century of research leading to understanding the scientific basis of selective mineral flotation and design of flotation collectors [J]. Mining, Metallurgy & Exploration, 2019, 36: 3−20.

[2] HUANG Zi-jie, WANG Jian-jun, SUN Wei, HU Yue-hua, CAO Jian, GAO Zhi-yong. Selective flotation of chalcopyrite from pyrite using diphosphonic acid as collector [J]. Minerals Engineering, 2019, 140: 105890.

[3] WEI Qian, JIAO Fen, DONG Liu-yang, LIU Xue-duan, QIN Wen-qing. Selective depression of copper-activated sphalerite by polyaspartic acid during chalcopyrite flotation [J]. Transactions of Nonferrous Metals Society of China,

2021, 31: 1784−1795.

[4] BUCKLEY A N, HOPE G A, LEE K C, PETROVIC E A, WOODS R. Adsorption of O-isopropyl-N-ethyl thionocarbamate on Cu sulfide ore minerals [J]. Minerals Engineering, 2014, 69: 120−132.

[5] MAREE W, KLOPPERS L, HANGONE G, OYEKOLA O. The effects of mixtures of potassium amyl xanthate (PAX) and isopropyl ethyl thionocarbamate (IPETC) collectors on grade and recovery in the froth flotation of a nickel sulfide ore [J]. South African Journal of Chemical Engineering, 2017, 24: 116−121.

[6] LIU Guang-yi, ZHONG Hong, DAI Tai-gen. The separation of Cu/Fe sulfide minerals at slightly alkaline conditions by using ethoxycarbonyl thionocarbamates as collectors: Theory and practice [J]. Minerals Engineering, 2006, 19: 1380−1384.

[7] MA Xin, XIA Liu-yin, WANG Shuai, ZHONG Hong, JIA Hui. Structural modification of xanthate collectors to enhance the flotation selectivity of chalcopyrite [J]. Industrial & Engineering Chemistry Research, 2017, 56: 6307−6316.

[8] CHEN Jian-hua. The interaction of flotation reagents with metal ions in mineral surfaces: A perspective from coordination chemistry [J]. Minerals Engineering, 2021, 171: 107067.

[9] SHERIDAN M S, NAGARAJ D R, FORNASIERO D, RALSTON J. The use of a factorial experimental design to study collector properties of N-allyl-O-alkyl thionocarbamate collector in the flotation of a copper ore [J]. Minerals Engineering, 2002, 15: 333−340.

[10] LI Yu-qiong, LIU Ying-chao, CHEN Jian-hua, ZHAO Cui-hua. Structure-activity of chelating collectors for flotation: A DFT study [J]. Minerals Engineering, 2020, 146: 106133.

[11] LIU Guang-yi, YANG Xiang-lin, ZHONG Hong. Molecular design of flotation collectors: A recent progress [J]. Advances in Colloid and Interface Science, 2017, 246: 181−195.

[12] NATARAJAN R, NIRDOSH I. Quantitative structure–activity relationship (QSAR) approach for the selection of chelating mineral collectors [J]. Minerals Engineering, 2008, 21: 1038−1043.

[13] YANG Fan, SUN Wei, HU Yue-hua. QSAR analysis of selectivity in flotation of chalcopyrite from pyrite for xanthate derivatives: Xanthogen formates and thionocarbamates [J]. Minerals Engineering, 2012, 39: 140−148.

[14] LIU Guang-yi, ZENG Hong-bo, LU Qing-ye, ZHONG Hong, CHOI Phillip, XU Zhenghe. Adsorption of mercapto-benzoheterocyclic compounds on sulfide mineral surfaces: A density functional theory study of structure–reactivity relations [J]. Colloids and Surfaces A: Physicochemical and Engineering Aspects, 2012, 409: 1−9.

[15] HU Yue-hua, CHEN Pan, SUN Wei. Study on quantitative structure–activity relationship of quaternary ammonium salt collectors for bauxite reverse flotation [J]. Minerals Engineering, 2012, 26: 24−33.

[16] TIAN Xiao-dong, LI Xue-ting, BI Peng-fei. Effect of O-isobutyl-N-ethyl thionocarbamates on flotation behavior of porphyry copper ore and its adsorption mechanism [J]. Applied Surface Science, 2020, 503: 144313.

[17] JIA Yun, HUANG Kai-hua, WANG Shuai, CAO Zhan-fang, ZHONG Hong. The selective flotation behavior and adsorption mechanism of thiohexanamide to chalcopyrite [J]. Minerals Engineering, 2019, 137: 187−199.

[18] HAN Guang, WEN Shu-ming, WANG Han, FENG Qi-cheng. Selective adsorption mechanism of salicylic acid on pyrite surfaces and its application in flotation separation of chalcopyrite from pyrite [J]. Separation and Purification Technology, 2020, 240: 116650.

[19] YIN Wan-zhong, SUN Qian-yu, LI Dong, TANG Yuan, FU Ya-feng, YAO Jin. Mechanism and application on sulphidizing flotation of copper oxide with combined collectors [J]. Transactions of Nonferrous Metals Society of China, 2019, 29: 178−185.

[20] ZHANG Xing-rong, LU Liang, ZHU Yang-ge, HAN Long, LI Cheng-bi. Research on the separation of malachite from quartz with S-carboxymethyl-O,O′-dibutyl dithiophosphate chelating collector and its insights into flotation mechanism [J]. Powder Technology, 2020, 366: 130−136.

[21] KHOSO S A, HU Yue-hua, LÜ Fei, GAO Ya, LIU Run-qing, SUN Wei. Xanthate interaction and flotation separation of H_2O_2-treated chalcopyrite and pyrite [J]. Transactions of Nonferrous Metals Society of China, 2019, 29: 2604−2614.

[22] LIU Sheng, LIU Guang-yi, HUANG Yao-guo, ZHONG Hong. Hydrophobic intensification flotation: Comparison of collector containing two minerophilic groups with conventional collectors [J]. Transactions of Nonferrous Metals Society of China, 2020, 30: 2536−2546.

[23] LI Shuang-ke, GU Guo-hua, QIU Guan-zhou, CHEN Zhi-xiang. Flotation and electrochemical behaviors of chalcopyrite and pyrite in the presence of N-propyl-N′-ethoxycarbonyl thiourea [J]. Transactions of Nonferrous Metals Society of China, 2018, 28: 1241−1247.

[24] PATRA A S, NULAKANI N V R, PAVAN K Y, SUBRAMANIAN V, DASH J, MUKHERJEE A K. Design and synthesis of novel polyamine collector to recover iron values from iron ore slimes [J]. Powder Technology, 2018, 325: 180−191.

[25] LIU Wen-bao, LIU Wen-gang, ZHAO Qiang, SHEN Yan-bai, WANG Xin-yang, WANG Ben-ying, PENG Xiang-yu. Design and flotation performance of a novel hydroxy polyamine surfactant based on hematite reverse flotation desilication system [J]. Journal of Molecular Liquids, 2020, 301: 112428.

[26] QIN Wei, XU Sheng-ming, XIE Qiang. Theoretical study of 2-mercaptobenzimidazole derivatives as chelating collectors in flotation separation of galena and pyrite [J]. International Journal of Mining Science and Technology, 2013, 23: 604−608.

[27] GEERLINGS P, de PROFT F, LANGENAEKER W. Conceptual density functional theory [J]. Chemical Reviews, 2003, 103: 1793−1874.

[28] FRISCH M J, TRUCKS G W, SCHLEGEL H B, et al. Gaussian 09 [M]. Revision A.03. Wallingford CT: Gaussian, Inc, 2009.

[29] THANIKAIVELAN P, SUBRAMANIAN V, RAO J R, NAIR B U. Application of quantum chemical descriptor in

quantitative structure activity and structure property relationship [J]. Chemical Physics Letters, 2000, 323: 59−70.
[30] LIU Guang-yi, ZHONG Hong, DAI Ta-gen, XIA Liu-yin. Investigation of the effect of N-substituents on performance of thionocarbamates as selective collectors for copper sulfides by ab initio calculations [J]. Minerals Engineering, 2008, 21: 1050−1054.
[31] LIU Guang-yi, ZHONG Hong, XIA Liu-yin, WANG Shuai, DAI Ta-gen. Effect of N-substituents on performance of thiourea collectors by density functional theory calculations [J]. Transactions of Nonferrous Metals Society of China, 2010, 20: 695−701.
[32] LIU Guang-yi, XIAO Jing-jing, ZHOU Di-wen, ZHONG Hong, CHOI P, XU Zheng-he. A DFT study on the structure-reactivity relationship of thiophosphorus acids as flotation collectors with sulfide minerals: Implication of surface adsorption [J]. Colloids and Surfaces A: Physicochemical and Engineering Aspects, 2013, 434: 243−252.
[33] HUANG Xiao-ping, HUANG Kai-hua, JIA Yun, WANG Shuai, CAO Zhan-fang, ZHONG Hong. Investigating the selectivity of a xanthate derivative for the flotation separation of chalcopyrite from pyrite [J]. Chemical Engineering Science, 2019, 205: 220−229.
[34] KHOSO S A, HU Yue-hua, LYU Fei, LIU Run-qing, SUN Wei. Selective separation of chalcopyrite from pyrite with a novel non-hazardous biodegradable depressant [J]. Journal of Cleaner Production, 2019, 232: 888−897.

新型铜硫浮选分离硫氨酯捕收剂的合成及吸附机理

曹 飞[1,2]，孙德四[1]，邱仙辉[3,4]，周德志[1]，张行荣[2]，孙传尧[2]

1. 九江学院 化学化工学院，九江 332005；
2. 矿冶科技集团有限公司 矿物加工科学与技术国家重点实验室，北京 102600；
3. 江西理工大学 资源与环境工程学院，赣州 341000；
4. 紫金矿业集团有限公司 低品位难选金矿综合利用国家重点实验室，上杭 364200

摘 要：设计合成一种新型铜硫浮选分离捕收剂：O-异丙基-N,N-二乙基硫代氨基甲酸酯(IPDTC)。先利用密度泛函理论计算 IPDTC 的电子结构。结果表明，IPDTC 比 O-异丙基-N-乙基硫代氨基甲酸酯(Z−200)具有更高的最高占据分子轨道能量和更低的电负性。根据相互作用能判据预测 IPDTC 具有较强的捕收能力。浮选试验表明，IPDTC 对黄铜矿和黄铁矿的捕收能力强于 Z−200。通过表面张力、吸附量、XPS、FTIR 和 zeta 电位等方法研究捕收剂的浮选机理。研究发现，IPDTC 可降低溶液表面张力。IPDTC 在黄铜矿表面的吸附能力强于黄铁矿，这与浮选试验结果相吻合。FTIR、zeta 电位和 XPS 结果表明，IPDTC 通过形成 Cu—S—C 键在黄铜矿表面发生较强的吸附作用，但在黄铁矿表面的吸附作用较弱。

关键词：O-异丙基-N,N-二乙基硫代氨基甲酸酯；吸附机理；黄铜矿；黄铁矿；密度泛函理论

(Edited by Bing YANG)